AFRL-AFOSR-UK-TR-2019-0021

Cell response determinants in laser-induced thermal impacts

Yoko Miura
Medizinisches Laserzentrum Lübeck GmbH
Peter-Monnik-Weg 4
Lübeck, 23562
DE

05/06/2019
Final Report

Air Force Research Laboratory
Air Force Office of Scientific Research
European Office of Aerospace Research and Development
Unit 4515 Box 14, APO AE 09421

REPORT DOCUMENTATION PAGE

Form Approved
OMB No. 0704-0188

1. REPORT DATE *(DD-MM-YYYY)*	2. REPORT TYPE	3. DATES COVERED *(From - To)*
05/04/2019	FINAL	09/15/2015-12/15/2018

4. TITLE AND SUBTITLE
CELL RESPONSE DETERMINANTS IN LASER-INDUCED THERMAL IMPACTS

5a. CONTRACT NUMBER

5b. GRANT NUMBER
FA9550-15-1-0443

5c. PROGRAM ELEMENT NUMBER

6. AUTHOR(S)
YOKO MIURA, RALF BRINKMANN

5d. PROJECT NUMBER

5e. TASK NUMBER

5f. WORK UNIT NUMBER

7. PERFORMING ORGANIZATION NAME(S) AND ADDRESS(ES)
MEDIZINISCHES LASERZENTRUM LUEBECK GMBH
PETER-MONNIK-WEG 4, 23562 LUEBCK, GERMANY

8. PERFORMING ORGANIZATION REPORT NUMBER

9. SPONSORING/MONITORING AGENCY NAME(S) AND ADDRESS(ES)
USAF, AFRL DUNS 143574726
AF OFFICE OF SCIENTIFIC RESEARCH
875 NORTH RANDOLPH STREET, RM 3112
ARLINGTON VA 22203-1954

10. SPONSOR/MONITOR'S ACRONYM(S)

11. SPONSOR/MONITOR'S REPORT NUMBER(S)

12. DISTRIBUTION/AVAILABILITY STATEMENT
APPROVED FOR PUBLIC RELEASE

13. SUPPLEMENTARY NOTES

14. ABSTRACT
In contrast to exogenous determinant of cell death (=temperature x time) following thermal stimulation, endogenous determinants turned out to be complexed and highly-regulated involving different proteins and molecules. Hsp70, which had been assumed to be one of the dominant determinants, also seems to be regulated by other different molecules such as VEGF and Thioredoxin, and calcium signaling appeared to be one of the key factors. We have established a real-time temperature measurement method for in-vitro cultures using optoacoustic technique. Using this method, mechanisms of temperature-resolved cell responses and determinants of subsequent cell functions could be investigated more in detaile.

15. SUBJECT TERMS
laser-induced hyperthermia, cell death determinants, heat shock protein, vascular endothelial growth factor, calcium signaling, optoacoustic temperature measurement, cell culture

16. SECURITY CLASSIFICATION OF:			17. LIMITATION OF ABSTRACT	18. NUMBER OF PAGES	19a. NAME OF RESPONSIBLE PERSON
a. REPORT	b. ABSTRACT	c. THIS PAGE			NANDINI IYER
U	U	U	UU	28	19b. TELEPHONE NUMBER *(Include area code)*

INSTRUCTIONS FOR COMPLETING SF 298

1. REPORT DATE. Full publication date, including day, month, if available. Must cite at least the year and be Year 2000 compliant, e.g. 30-06-1998; xx-06-1998; xx-xx-1998.

2. REPORT TYPE. State the type of report, such as final, technical, interim, memorandum, master's thesis, progress, quarterly, research, special, group study, etc.

3. DATE COVERED. Indicate the time during which the work was performed and the report was written, e.g., Jun 1997 - Jun 1998; 1-10 Jun 1996; May - Nov 1998; Nov 1998.

4. TITLE. Enter title and subtitle with volume number and part number, if applicable. On classified documents, enter the title classification in parentheses.

5a. CONTRACT NUMBER. Enter all contract numbers as they appear in the report, e.g. F33315-86-C-5169.

5b. GRANT NUMBER. Enter all grant numbers as they appear in the report. e.g. AFOSR-82-1234.

5c. PROGRAM ELEMENT NUMBER. Enter all program element numbers as they appear in the report, e.g. 61101A.

5e. TASK NUMBER. Enter all task numbers as they appear in the report, e.g. 05; RF0330201; T4112.

5f. WORK UNIT NUMBER. Enter all work unit numbers as they appear in the report, e.g. 001; AFAPL30480105.

6. AUTHOR(S). Enter name(s) of person(s) responsible for writing the report, performing the research, or credited with the content of the report. The form of entry is the last name, first name, middle initial, and additional qualifiers separated by commas, e.g. Smith, Richard, J, Jr.

7. PERFORMING ORGANIZATION NAME(S) AND ADDRESS(ES). Self-explanatory.

8. PERFORMING ORGANIZATION REPORT NUMBER. Enter all unique alphanumeric report numbers assigned by the performing organization, e.g. BRL-1234; AFWL-TR-85-4017-Vol-21-PT-2.

9. SPONSORING/MONITORING AGENCY NAME(S) AND ADDRESS(ES). Enter the name and address of the organization(s) financially responsible for and monitoring the work.

10. SPONSOR/MONITOR'S ACRONYM(S). Enter, if available, e.g. BRL, ARDEC, NADC.

11. SPONSOR/MONITOR'S REPORT NUMBER(S). Enter report number as assigned by the sponsoring/ monitoring agency, if available, e.g. BRL-TR-829; -215.

12. DISTRIBUTION/AVAILABILITY STATEMENT. Use agency-mandated availability statements to indicate the public availability or distribution limitations of the report. If additional limitations/ restrictions or special markings are indicated, follow agency authorization procedures, e.g. RD/FRD, PROPIN, ITAR, etc. Include copyright information.

13. SUPPLEMENTARY NOTES. Enter information not included elsewhere such as: prepared in cooperation with; translation of; report supersedes; old edition number, etc.

14. ABSTRACT. A brief (approximately 200 words) factual summary of the most significant information.

15. SUBJECT TERMS. Key words or phrases identifying major concepts in the report.

16. SECURITY CLASSIFICATION. Enter security classification in accordance with security classification regulations, e.g. U, C, S, etc. If this form contains classified information, stamp classification level on the top and bottom of this page.

17. LIMITATION OF ABSTRACT. This block must be completed to assign a distribution limitation to the abstract. Enter UU (Unclassified Unlimited) or SAR (Same as Report). An entry in this block is necessary if the abstract is to be limited.

MEDICAL LASER CENTER LÜBECK

Non-profit Research & Development Company

Final Performance Report

Grant Number: FA9550-15-1-0443

Title:

"Cell Response Determinants in Laser-Induced Thermal Impacts"

PI: Dr. Yoko Miura, Dr. Ralf Brinkmann

Period of Performance: 16. Sep. 2016 - 15. Dec. 2018

AFOSR PM: Dr. Nandini Iyer, Email: nandini.iyer.2@us.af.mil
CFDA Number: 12.800
PI: Yoko Miura, M.D., Ph.D.
Co PI: Ralf Brinkmann, Ph.D.
Organization: Medizinisches Laserzentrum Lübeck GmbH
DUNS number: 320953250
NATO CAGE number: DL328

SAM Registration: MLL GmbH
Address: Peter-Monnik-Weg 4, 23562 Lübeck, Germany
Phone PI: + 49-451-3101-3212 **FAX:** + 49-451-3101-3204
E-mail PI: miura@bmo.uni-luebeck.de
Country: Germany

Lübeck, May 4th, 2019

CONFIDENTIAL

Contents

1. List of figures

2. Project progress overview

The project was initiated with the works for the working packages 3-5 in the first year (Sep 2015- Sep 2016). In the second year (Sep 2016-Sep 2017), the working package 1 has been started and the first original model was completed in 2018. Regarding working package 2, the visit of our researcher to the laboratory of Dr. Denton in AFRL was realized at the end of October, and two different techniques were compared. The works for the working packages 4 and 5 were continuously performed in the third year, in order to elucidate different aspects of laser-induced hyperthermia-resolved cell responses.

Working package **1**: In vitro optoacoustic temperature measurements on RPE hyperthermia model

Working package **2**: Investigation of the accuracy of temperature measurement with two different techniques

Working package **3**: Investigation of damage kinetics after thermal laser irradiation

Working package **4**: Investigation of intracellular signaling and proteostasis after thermal laser irradiation

Working package **5**: Investigation of long-term cellular functionality after thermal laser irradiation

	1st year (Sep. 15-Sep.16)				**2nd year (Sep.16-Sep.17)**				**3rd year (Sep.17-Sep.18)**				**Sep.18-Dec.18**
	Q1	**Q2**	**Q3**	**Q4**	**Q5**	**Q6**	**Q7**	**Q8**	**Q9**	**Q10**	**Q11**	**Q12**	**Q13**
WP1													
WP2													
WP3													
WP4													
WP5													

3. Report of the third project year (plus extended 3 months) (Sep. 2017-Dec. 2018)

WP1: In vitro optoacoustic temperature measurements on RPE hyperthermia model
(Published manuscript: Miura et al.“ Real-time optoacoustic temperature determination on cell cultures during heat exposure: a feasibility study” *International Journal of Hyperthermia*. 36:1,466-472)

3.1.1. Purpose:

The aim of this work is to employ the optoacoustic technique for two-dimensional temperature measurements in cell cultures during exposure to a second laser that generates localized hyperthermia. Here we report our method and setup, with the first proof-of-concept results in an in vitro model consisting of RPE cells.

3.1.2. Materials and Methods

3.1.2.1. Measurement setups

A schematic drawing of the experimental setup is shown in Figure 1. A continuous wave thulium laser (TLR-20, IPG Laser GmbH, Burbach, Germany) emitting a wavelength of 1.94 µm is delivered from below to heat cells on the glass bottom surface of the culture dish, as well as the aqueous solution above the cells. The light is guided via an optical fiber (core diameter of 365 mm, NA of 0.2; StarMedTec GmbH, Starnberg, Germany). A plan-convex quartz lens (f=50mm) is located 50 mm behind the fiber and 150 mm prior to the cell culture dish, having a 170 µm-thick IR-transparent glass (D 263 M Schott AG, Mainz, Germany). The light is projected to the cell culture dish with a radius of 5.2 mm. mThe lateral beam profile was approximately Gaussian. A self-developed Q-switched holmium laser, emitting a wavelength of 2.1 µm, served as the probe laser for determining the temperature of cells and medium optoacoustically. Its pulse duration was set to 60 ns, the repetition rate to 100 Hz, and the maximum pulse energy available in the plane of cells was 134 µJ. The probe beam spot, with a diameter of less than 1 mm, was scanned with a

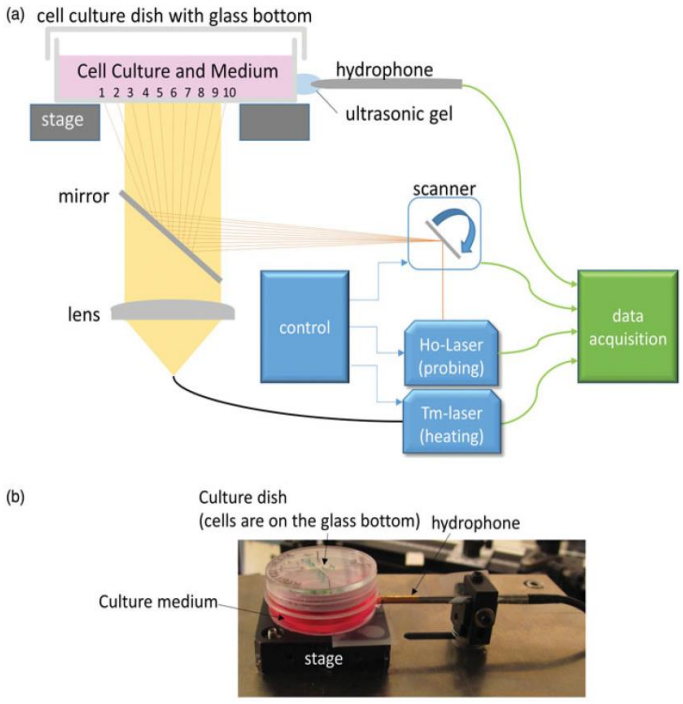

Fig. 1. (a) A schematic drawing of the heating/measurement setup. (b) A picture of a cell culture dish with a culture medium (with phenol red) and a hydrophone. {Miura, 2019 #15}

galvo scanner (GCM001, Thorlabs Inc., Newton, MA) in a line over the whole diameter (20 mm) of the cell growingarea in a culture dish with a scan frequency of 10 Hz. Thus, 10 equally spaced (2 mm) spots, center to center, were addressed by each scan. This means that for each spot, temperature is acquired every 100 ms. For pulse energy stability reasons, the holmium laser is operated permanently while its emission on the sample is controlled by a shutter (SH05, Thorlabs Inc.) in the optical path. A dichroic mirror (HR coating 1850–2130, Layertec GmbH, Mellingen, Germany) combines both laser beams. In order to detect the ultrasonic pressure waves after the holmium laser impact, a hydrophone (PZT-Z44-1500, ONDA, Sunnyvale, CA) was located outside the dish. Ultrasonic gel was used to enable acoustic coupling. The ultrasonic pressure waves were amplified by a preamplifier (Olympus 56605B, 60 dB; 20 kHz–2 MHz). A PC-based digitizer (GaGe/Dynamic Signals LLC, Lockport, NY) with a sampling rate of 200 MHz and a resolution of 14 bit was used for digitizing. The energy of each pulse was measured by integrating over the pulse power measured with a fast photodiode (J23-18I-R250U-2.2, Laser Components GmbH, Olching, Germany). The OA pressure transient received by the hydrophone was rectified and numerically integrated over the time of high amplitudes in order to improve the signal to noise ratio. For laser irradiation on cell cultures, a confluent RPE cell culture with 3.5 ml culture medium was placed on the irradiation stage. The baseline of the medium temperature was room temperature (about 23 °C). A co-aligned aiming beam (k=635 nm, max power 1 mW) allowed positioning of the irradiation laser within the culture dish. Three seconds after the start of the scanner and the probe laser, the heating laser was turned on for a 10-s irradiation with a laser power of either 0 W (control), 2.8 W, or 6.0 W. The water absorption coefficients at thulium (1.94 µm) and holmium (2.1 µm) laser wavelengths are 12.8 mm^{-1} and 2.86 mm^{-1} with 1/e penetration depths of 78 µm and 350 µm, respectively.

3.1.2.2. OA Temperature determination

The principle for OA temperature determination is based on thermoelastic expansion after short pulsed heating. The amplitude of the emitted pressure wave is proportional to the absorbed pulse energy Ep and the temperature-dependent Grüneisen coefficient C (T). The Gr€uneisen coefficient of water is well approximated by a second order polynomial in the range of 10–90 °C relevant for this work. The required values can be found in the literature [16], with a zero-crossing p(T)=0 at T0=4 °C and a maximum dP/dT=0 at T_{max}=121°C. In the case a laser pulse is used to measure water temperature with constant temperature over the penetration depth of the laser radiation, the optoacoustically evaluated temperature T_{OA} can be expressed as follows:

$$T_{OA}(T) = T_{max} - \sqrt{(T_{max} - T_0)^2 + \frac{p(T)}{S \cdot E_p}}$$

where p(T) represents the pressure at temperature T. The proportionality constant, S, is determined for every scan position separately, prior to heating with the thulium laser, by normalizing the pressure $p(T_{amb})$ to the ambient temperature $T_{amb}=T_{OA}$. For T_{OA} verification, a thermocouple (ALKB025, Rössel Messtechnik GmbH, Dresden, Germany) was placed in the medium at the center of the cell culture dish, very close to the dish bottom. Temperature data were digitized (NI9211, National Instruments, Austin, TX) and stored to be compared with T_{OA}.

3.1.2.3. RPE cell culture and cell viability assay after laser irradiation

RPE cell culture: As described in the annual report of last year. The primary porcine RPE culture at the second passage was used in experiment.

Viability test (MTT assay) after laser irradiation

Primary porcine RPE cells were cultured in a Dulbecco's Modified Eagle Medium (DMEM, high glucose, Sigma-Aldrich), supplemented with 10% porcine serum, 1mM sodium pyruvate, 100 unit/ml penicillin and 0.1 mg/ml streptomycin. Cells were maintained in an incubator at 37°C under 5% CO_2. Confluent second passage cell cultures (approximately $4x10^5$ cells/dish) on glass-bottom dishes (m-Dish 35 mm, growth area: diameter of 20 mm, ibidi) were used for experiments. Three hours after laser irradiation, the culture medium was replaced by 1ml of 3–(4,5-dimethylthiazol-2-yl)-2,5 diphenyltetrazolium bromide (MTT) solution (1.25 mg/ml) and incubated for 2 h to be converted to a formazan product in the mitochondria of healthy cells. The MTT solution was removed and features of the cell cultures were documented using digital photography from above the dishes. Images of the entire cell growth area (20mm diameter) enabled a visual inspection for cell coverage (confluence), staining by MTT, homogeneity of purple pigmentation, as well as laser-dependent damage (lack of MTT stain). To estimate the extent of cell damage in the cultures, a 1mm grid paper was placed beneath the dish during imaging. To quantify the MTT conversion by healthy cells, 2 ml of dimethyl sulfoxide (DMSO) were added to each dish to dissolve the formazan product. After 30 min, absorbance of the DMSO-formazan solution was measured at 570 nm using a photometer (SpectraMax M4, Molecular Device). The absorbance value is a direct estimate of the number of live cells after laser exposure.

3.1.3. Results:

3.1.3.1. Verification of the method

Fig. 2 shows the temperature decay curves for the validation experiment, where the OA and thermocouple measurements were carried out with pre-warmed medium (52°C) in a dish during cooling down (to 35°C). The mean value of the T_{OA} from 10 different measure positions at each point in time is shown with the solid black line, and the average standard deviation as dash lines (2.3 ± 2.1°C).

The reference temperature via thermocouple measurement, shown with the blue line, is within the standard deviations of T_{OA}. This proves the validity and accuracy of the OA method compared to the standard temperature measurement by a thermocouple.

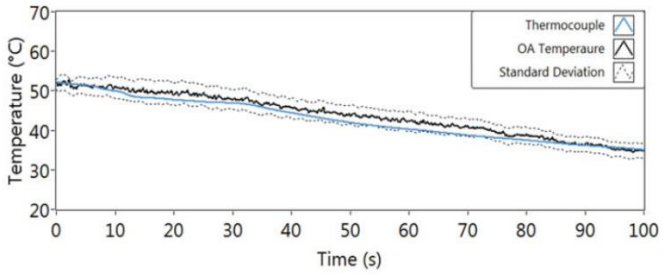

Fig. 2. The temperature, measured by a thermocouple (reference temperature, blue line), and the simultaneously obtained T_{OA} (black solid line, standard deviation with black dash lines) of the culture medium during cooling from about 52°C to 35°C. {Miura, 2019 #15}

3.1.3.2. Temperature measurement on RPE cell culture during laser heating

The measured temperature rises over time for each scan position are shown in Figure 3. The OA-temperature acquisition was stopped after 30 s. It was shown that the probe laser alone does not lead to a measurable temperature rise of the medium (Figure 3 (a)). The exposure with the thulium laser power of 2.8W induced temperature increases above 40 _C at several scan positions close to the center of the dish (Figure 3 (b)). Increasing the power of the heating laser to 6W led to temperatures of around 50°C (Figure 3 (c)).

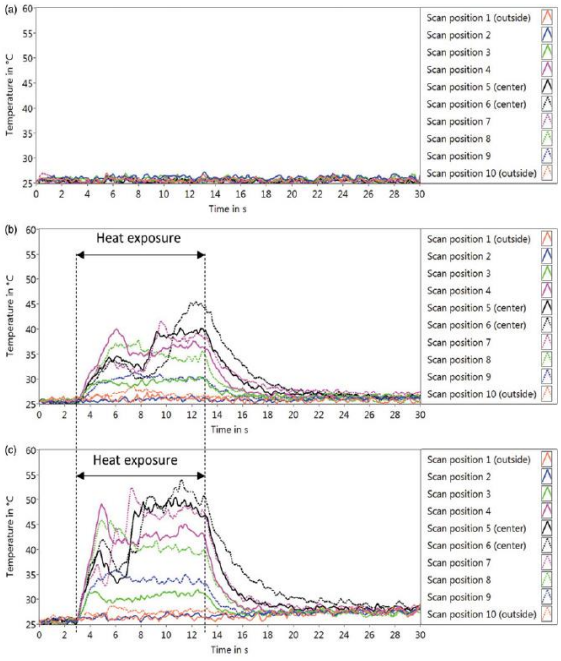

Fig. 3: Optoacoustic temperatures (T_{OA}) at each position on RPE cell culture over time during laser heating, with the laser power of 0W (only probe laser) (a), 2 W (b), and 6.8 W (c). About 3 s after the probe laser and the scanner were started, the heating laser was turned on followed by the 10-s irradiation ('Heat exposure'). The temperature measurements (10 Hz) were continued until 30 s. The temperature course of each measurement point is plotted with different colors and styles.{Miura, 2019 #15}

3.1.3.3. Temperature distribution over the cell culture dish

The temperature distributions across the culture dish during the last second (10th second) of laser irradiations are plotted and shown in Figure 4 (panels a-c). The peak temperature near the center of the dish was 44°C when exposed to 2.8 W (Figure 4 (c)), and 51 °C when exposed to 6 W (Figure 4 (e)).

Several features are shown in the color images (Figure 4 (b, d, f)) of the MTT stained cell cultures 3 h post laser exposure. The uniform distribution of purple color (MTT-formazan) in panels (b) and (d) indicates similar confluence of the cell monolayers, and that no photothermal damage took place. The striking loss of purple color in Figure 4 (f) indicates the central higher temperature (max 51°C) through 6 W laser exposure damaged a large area of the cell monolayer and could not transform the MTT to the formazan product. The round nature of the damaged area in panel f shows that the varied pigmentation did not alter the bulk water heating by the heating laser.

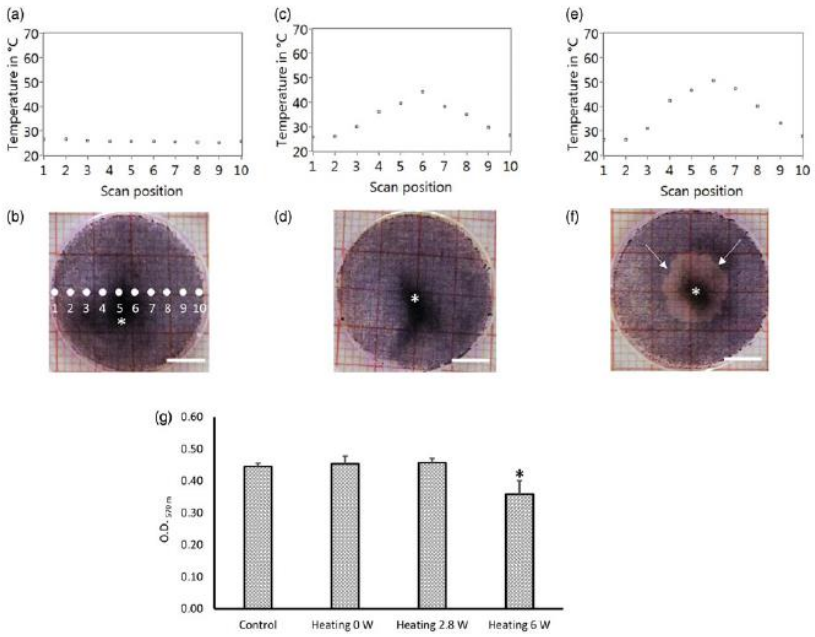

Fig. 4. T_{OA}-distribution across the culture dish bottom at the 10th second of irradiation (a, c, e), and the results of MTT assay (cell viability test) for corresponding cell cultures (b, d, f), with the heating laser power of 0W (only probe laser) (a, b), 2 W (c, d), and 6.8 W (e, f). The pictures (b, d, f) are the digital photography images of the cell culture with formazan before lysed. Asterisk (*) shows the inhomogeneous melanin pigmentation. Arrows in (f) indicate the boundary between live and dead cells. (g) The quantification of formazan of the cell lysis by measuring the light absorption at 570 nm. Bar = 5 mm. {Miura, 2019 #15}

3.1.3.4. Discussion/Conclusion

In this work, we achieved to build a non-contact method to acquire the temperature rise of cells in a cell culture dish when heating them by laser exposure with a wavelength well absorbed by water.

To further verify the OA-temperature method at the cell level, a combination with thermal imaging with an IR-thermocamera would allow comparisonm, because the two methods do not interfere with each other. We could add two more hydrophones to improve the signal/noise ratio, but it requires another data equision board.
In conclusion, this method could find a wide application for studying hyperthermia or other temperature related cellular effects with high spatial and temporal resolution without using contacting thermocouples or an IR-thermocamera. Finally, the method could also be extended to other models and materials.

For more detail, please see our publcation attached:
"Real-time optoacoustic temperature determination on cell cultures during heat exposure: a feasibility study". International Journal of Hyperthermia, 36:1,466-472, DOI: 10.1080/02656736.2019.1590653
https://tandfonline.com/doi/pdf/10.1080/02656736.2019.1590653

3.2. WP.2: Investigation of the accuracy of temperature measurement with two different techniques

In order to investigate the possibility and accuracy to measure temperatures on cell cultures by means of the optoacoustic (OA) effect making use of the temperature dependent thermoelastic expansion, proof-of-concept experiments were carried out in October 2017 at the US Airforce Research Laboratory at Fort Sam Houston, San Antonio, Tx in the group and under supervision of Michael Denton in the Bioeffects division. For a first proof-of-concept a complex setup was realized to irradiate and probe cells in a culture dish by use of a cw laser for heating and a pulsed laser for probing, while simultaneously the culture dish was observed with a high speed IR-camera in order to read out the temperature rise with high spatial and temporal resolution. A high bandwidth needle hydrophone and the OA processing software developed at MLL were implemented. The main components for the setup:

1. Heating laser: Positive Light Inc: repetition rate: wavelength: 527 nm; pulse duration: 300 ns, repetition rate: 1 kHz, pulse energy: 30 – 50 µJ; spot size on sample: 60 µm
2. Temperature probe laser: Spectra Physics Inc, Model Millenia XsJS, wavelength: 532 nm; power in continuous wave mode: 0.2 – 10 W, fiber coupled application onto a spot size on sample: 300 µm
3. IR-camera: FLIR Systems SC4000; frame rate 800 Hz, 192*192 px, detected area: 1.6*1.6 mm²

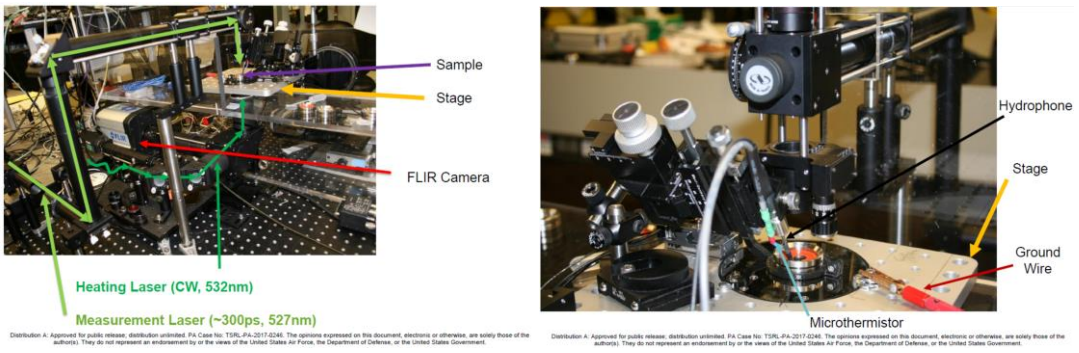

Fig. 5. Overview of the setup and in more detail of the probing area with integrated hydrophone and microthermistor for calibration and background temperature determination. left side: Setup with the main components, right side: probing area with cell culture dish, attached hydrophone and microthermistor for the validation experiment

Figure 5 shows an overview of the setup and in more detail of the probing area with integrated hydrophone and microthermistor for calibration and background temperature determination. The probe laser area with a diameter of 60 µm was placed in the center of the heating area of 300 µm, thus just the central and maximal temperature in the middle of the culture dish was probed by optoacoustics, while the IR camera recorded a large field of view of 1.6*1.6 mm². Heating was performed for 75, 325 and 955 ms. For

acoustic probing, the raw data of the hydrophone with central frequencies around 30 MHz were processed according to the following flow chart:

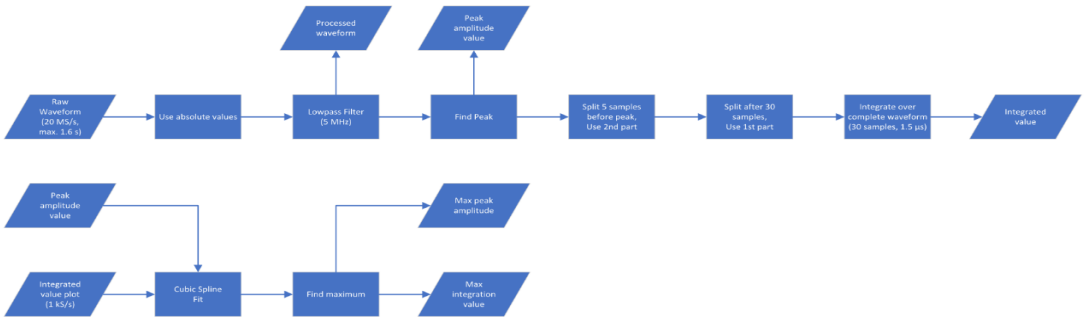

Fig. 6. Flow chart for processing the optoacoustic data from the raw acoustic transients to the OA integrated value, which is calibrated on the temperature as shown in Fig. 7

As target, by melanin phagocytoses artificially pigmented RPE cells were used, which can be heated by green laser light owing to the broad absorption of melanin in the visible spectrum. The calibration curve for thermoelastic expansion of the melanin samples was been recorded prior to time dependent experiments by laser heating with powers between 17.5 and 208 mW, and gathering the temperature by the IR camera at the end of the heating period. In Figure 7 the OA-amplitudes as calculated according to the flow chart shown in Figure 6, were plotting over the temperature recorded with the IR camera at the end of the heating period, exemplary after 975 ms as shown. The dependency can be approximated by a second order harmonics as for RPE organ cultures, however, the extrapolated transition through the temperature axis was found at -33 °C, which is slightly higher than for pigmented organ cultures (-17°).

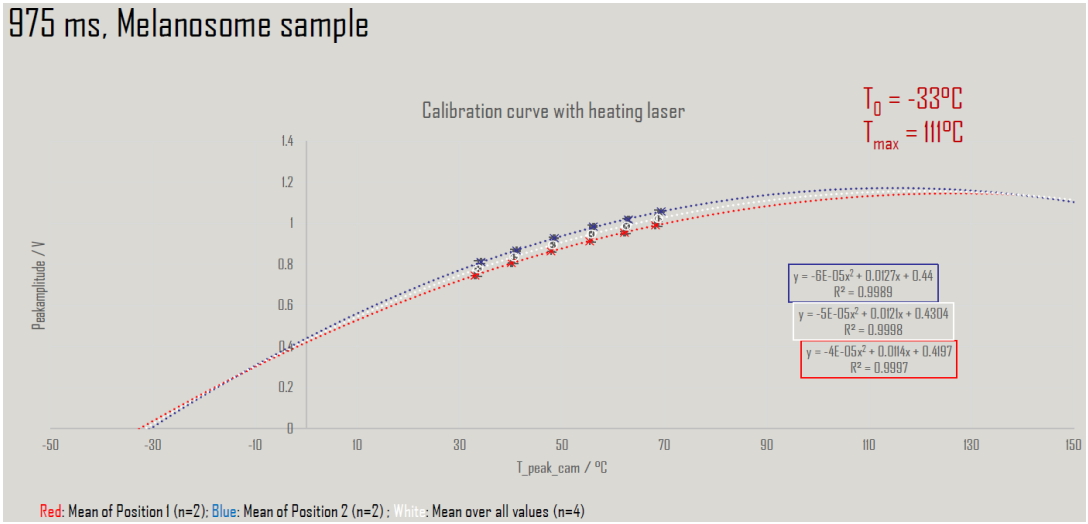

Fig. 7: Calibration curve of temperature-dependent OA-amplitudes determined as shown in Fig. 6.

Using the calibration curve, time dependent measurements were conducted in order to compare the temperature slope of both measurement techniques (OA and thermo-camera). A typical result is shown in Figure 8 with the thermogram of the thermocamera in an en-face view at the end of a 955 ms irradiation, showing a radial temperature distribution across the culture dish as expected. The transducer output shows the typical logarithmic temperature rise as expected, however, the signal to noise ratio (SNR) is around 20 % peak to average and 5 % rms over 1 second. Overlaying the temperature rise of the thermos-camera with the OA-data using the calibration curve as shown in Figure 7, a similar course is obtained. Similar results were obtained for the shorter heating times.

However, the average slope is slightly lower with the OA technique compared to the central IR course. This deviation is expected since the OA data display an average temperature rise over the probed area of 60 µm in diameter, while the thermal camera shows exactly the maximum value at the center. The deviation is result of the radial temperature drop owing to heat diffusion which becomes stronger the longer the heating takes place. However, the average OA temperature rise can be recalculated to obtain the maximum value as it has already been done for temperature calculations at the retina by a mathematical transient smoothing function.

In conclusion, these first proof-of-concept experiments to determine temperatures rise on artificially pigmented cells during heating with OA techniques reveals promising results. The comparison with an accurate but elaborate method using a high speed IR-

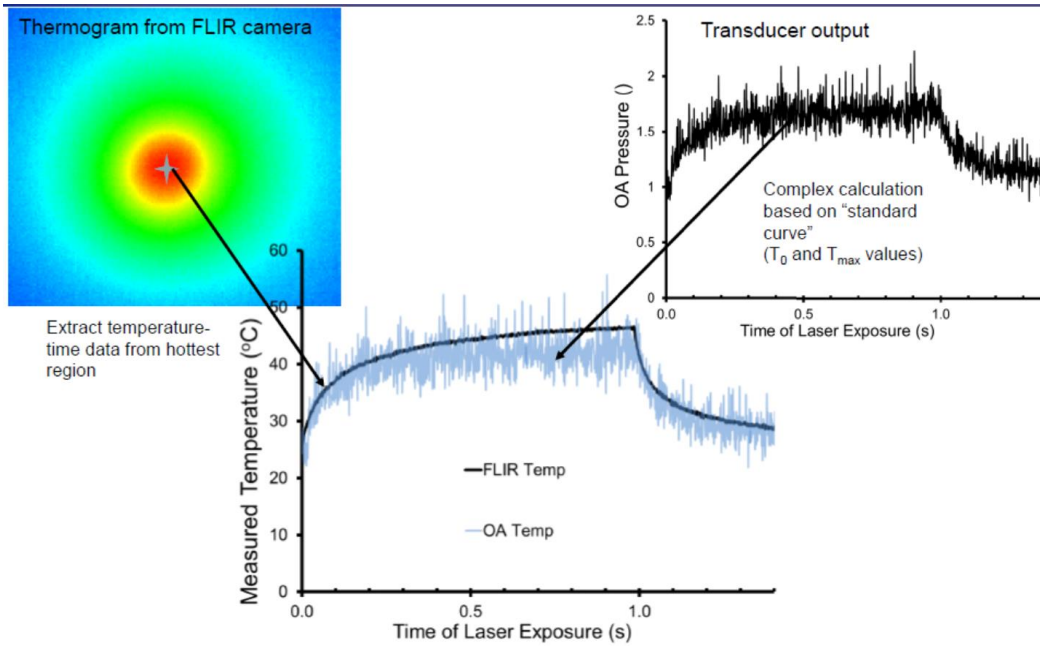

Fig. 8. Lateral Temperature distribution over the cell culture dish (top left), OA pressure amplitude as an average over the central 60 µm diameter and temperature curses over time for the 955 ms heating period and following cool down time

thermal camera proved that OA temperature measurements with a simple hydrophone and a Q-switched probe laser reveals similar temperature slopes. As expected the calibration curves need to be adapted to the different cells and environment, however, which also counts for the IR technique. The OA-temperature accuracy for the average temperature rise is around few degrees, however, so far comparing an average spatial temperature rise with a punctual rise. In further work the average temperature needs to be converted to the maximum temperature, as already been done for organ cultures, rabbit as well as human eyes, with a mathematical smoothing curve. Further experiments should also be conducted to optimize the equipment and improve the SNR. One major pint here is to normalize the OA transients on the energy of every single laser pulse of the Q-switch probe laser, since the OA pressure is directly proportional to the laser pulse energy. This will significantly improve the deviations as shown in Fig. 8, thus reducing the SNT and strongly improve the temperature accuracy.

3.3. WP4: Investigation of intracellular signaling and proteostasis

3.3.1.Summary of last years:

The purpose of these part of the project is to elucidate the determining factors for heat-induced cell death and possible intracellular pathways following heat stimulations. Last years, we investigated the threshold temperature for cell death, type of cell death (necrosis and apoptosis), expression of Hsp70, influence of Hsp70 inhibition during laser irradiation on cell survival, role of thermos-sensitive TPRV1 channel, and expression and secretions of growth factors such as VEGF and PEDF.

3.3.2. Effect of inhibition of VEGF-R2 on response of cultured PRE cells to laser-induced sublethal hyperthermia

In the third year, we have investigated the effect of an inhibitor of VEGF-R2 (VEGF receptor 2) on cell survival after hyperthermia and protein expressions, in order to have deeper insights into the regulation between Hsp70 and VEGF-A/VEGFR2 signaling stimulated by heat.

3.3.2.1. Background/state of the art

VEGF-A/VEGFR2 signaling pathway is known to be responsible for angiogenesis and of neovascular retinal diseases (Fig. 9),[1] and thus antibodies of VEGF-A are utilized to treat patients with neovascular retinal diseases, such as age-related macular degeneration.[2]
VEGF-A/VEGFR2 is, however, also known as an autocrine survival factor for RPE cells.[3] Recent study has reported that repetitive anti-VEGF treatment may induce atrophy of RPE.[4] Therefore attempts are being made to reduce the number of injection of anti-VEGF agents.
One of the alternative/adjunct treatment is the laser-induced sublethal thermal laser treatment. Results of several clinical studies have shown that combination of weak to sublethal retinal laser irradiation may significantly decrease the number of anti-VEGF injection with the patients of macular edema.[5]
However, very importantly, the influence of the inhibition of VEGF-A/VEGFR2 signaling using anti-VEGF agents on RPE cell responses to sublethal hyperthermia is not known to date. The association between VEGF-A/VEGFR2 signaling and expression and function of heat shock protein (Hsp) 70, one of the important heat-induced proteins, has not been elucidated so far to date.

In this study, we have investigated the association between VEGF-A/VEGFR2 signaling and Hsp70 expression, especially after sublethal hyperthermia.

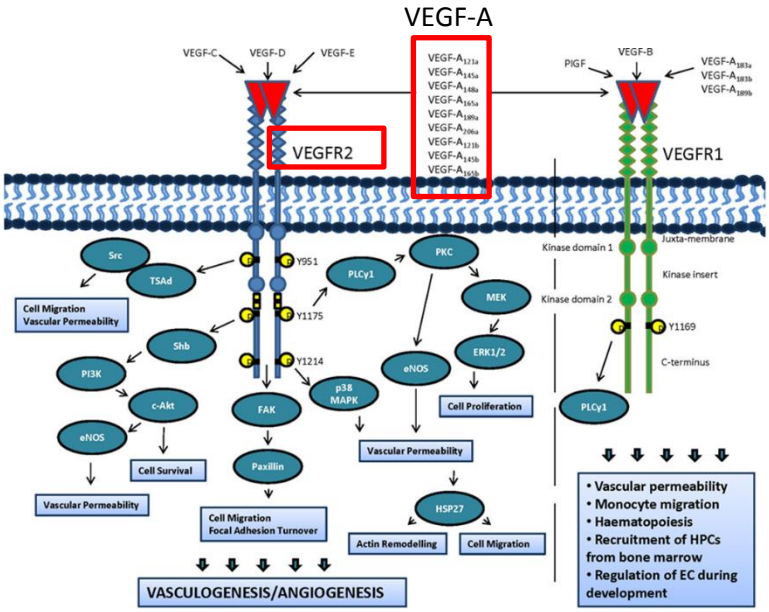

Fig. 9: VEGFR1 and VEGFR2 and their associated ligands
Fearnley GW, Smith GA, Harrison MA, Wheatcroft SB, Tomlinson DC, Ponnambalam S. Vascular endothelial growth factor-A regulation of blood vessel sprouting in health and disease. OA Biochemistry 2013 Feb 01;1(1):5.

3.3.2.2. Materials and Methods

i. RPE cell culture

As described in the annual report of last year. The primary porcine RPE culture at the second passage was used in experiment.

ii. Cell heating with thulium laser

As described in the annual report of last year.

An experimental setup containing a thulium laser (Vela, Starmedtec GmbH, Germany, wavelength 1940 nm, power range 0-20 W) was used. The laser spot diameter at cellular level is fixed to 30 mm, which is equivalent to the inner diameter of the cell culture dish. Duration of irradiation was fixed to 10s.

One hour before irradiation cell culture medium was replaced with the 37 °C-pre warmed 1200 µL fresh medium. The 10s-irradiation was performed with pre-determined power-setups so that the T_{10s} at the center of the culture dish (T_{max}) reaches about 40, 43, 47, 51 and 59 °C (2.7 W for 40 °C, 4.9 W for 44 °C, 7.7 W for 47 °C, 10.4 W for 51 °C and 15.9 W for 59 °C). After irradiation, the culture dish was placed back to the incubator and kept until used for further examinations. The temperature distribution at the 10th second of irradiation is shown in Fig.10.

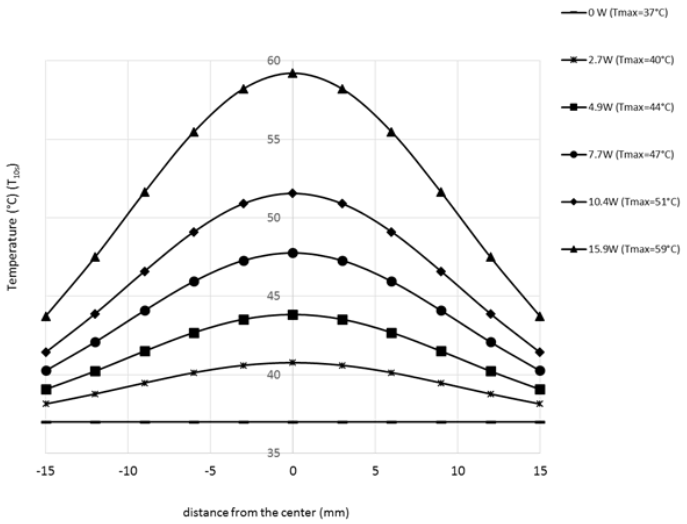

Figure 10 : Temperature distributions at the 10th second across the culture dish.

iii. Inhibition of VEGFR2-signaling

An antibody of VEGFR2/KDR/Flk-1 (R&D System, MAB3572) was used to inhibit function of VEGFR2. It has been already shown that this antibody can inhibit VEGF-dependent endothelial cell proliferation.[6] Since the lethal dose for cultured RPE was not known, toxicity test was performed in advance with MTT assay and examined concentration of the antibody was determined to 40 ng/ml.

The culture medium was replaced by VEGFR2/KDR/Flk-1 antibody (40 ng/ml)-containing medium 2h before irradiation. Two hours later the cells were irradiated as described above. The cell viability, VEGF secretion, intracellular amount of Hsp70, was investigated at 3h and 24h after irradiation.

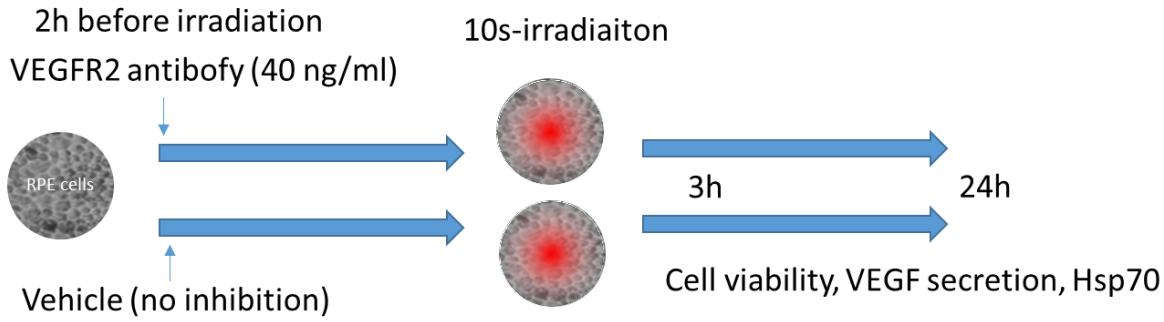

Fig. 11: Schematic study flow to investigate the effect of anti-VEGFR2

iv. Immunocytochemistry for VEGFR2 in cultured RPE cells

To confirm the existence of VEGFR2 in cultured RPE cells, immunofluorescence staining was performed. The cells were washed once with ice cold PBS, fixed with 3.7% PFA for 15 minutes, washed three times with PBS and then permeabilized with 0.05% Triton-X 100. The cells were blocked using 1% BSA solution in PBS. Incubation with a mouse anti-VEGFR2- antibody (the same product as used to inhibit the function; 40 ng/ml) was carried out overnight at 4°C. After three washing steps with PBS the cells were incubated with the secondary antibody Goat-anti-mouse-AlexaFluor 532 for one hour at room temperature. Nuclear DNA was stained using DAPI. F-actin was stained with FITC-Phalloidin. Mounting was performed using 1.5 ml PBS. Immunofluorescence was documented at a fluorescence microscope (Eclipse Ti, Nikon, Tokyo, Japan).

v. Measurement of extracellular VEGF-A under VEGFR2 inhibition (ELISA)

Secretion of VEGF from cultured RPE cells into the medium was investigated using ELISA. Culture supernatant was collected and centrifuged at about 1000g for 10 min to remove cell debris. The supernatant was then stored in -20°C until use. VEGF ELISA was conducted using commercially available kit (Human VEGF Quantikine ELISA kit, R&D system, Minneapolis, MN) according to the manufacturer's introduction.

vi. Cell viability under VEGFR2 inhibitor (Flow cytometry)

At 3 and 24h after laser irradiation, the cell culture supernatant of each sample was collected separately in a 1.5 ml Tube. The cells were then treated with 300 µl Trypsin/ EDTA for 5 min, and collected into the tube with corresponding supernatant. The cell suspension was centrifuged at 9600g for 7 min, the supernatant was discarded, and the cell pellet was resuspended in 1 ml PBS. After another centrifugation at 9600g for 7 min the cells were re-suspended in 300 µl assay buffer. 100 µl of each sample were pipetted in FACS Tubes and 5 µl ethidium homodimer-III (EthD-III) (for dead cells;10 µg/ml) as well as FITC-annexin-V (for apoptotic cells; 50 µg/ml) were added. The suspensions were incubated for 15 min under dark, and then 400 µl assay buffer were added.

Flow cytometry analysis was conducted with a FACScan (Becton Dickinson, San Jose, USA). The laser used to excite fluorophore is 488 nm.

Filter name	Excitation laser (nm)	Bandpass filter (nm)
FITC-Filter (for FITC-Annexin-V)	488	530 ±15
TRITC-Filter (for EthD-III)	488	585 ± 21

vii. Intracellular amount of heat shock protein 70 (Hsp70) under VEGFR2 inhibitor after laser-induced hyperthermia (western blotting)

Principally the method to detect protein is also same as stated in the annual report of last year.

Cell lysis

Cells were lysed at different time points (3, 24h) after irradiation using RIPA Lysis Buffer System (Santa Cruz Biotechnology Inc.). Lysis was carried out as recommended by the manufacturer.

Measurement of total protein amount (Bradford protein Assay)

Bradford Assay was performed to measure the total protein concentration after cell lysis using Bio-Rad Protein Assay Dye Reagent Concentrate (Bio-Rad Inc.). BSA dilutions were used as protein standard. Detection of absorbance was performed at 595 nm wavelength in Spectramax M4 (molecular devices, Sunnyvale, USA).

Electrophoresis and western blotting

The samples containing 50 µg protein (sample Volume 25 µl, containing water, Bromophenol blue, ß-mercaptoethanol, and cell lysate) were boiled at 95°C for 5 min. Electrophoresis was conducted using 4–15% Mini-PROTEAN® TGX Stain-Free™ Protein Gels (10 well, 30 µl, Bio-Rad Laboratories), the transfer of the proteins from the SDS-Gel to the PVDF-Membrane was executed using the Trans-Blot® Turbo™ Transfer System (Bio-Rad Laboratories). PVDF-membranes were activated by incubation in 90% EtOH for 1 min; afterwards filter papers and PVDF-membranes were equilibrated in transfer buffer (Trans-Blot Turbo transfer buffer containing EtOH). The blotting stacks were build (2x filter papers, membrane, gel, 2x filter papers) and the blotting was performed according to the protocol of the Trans- Blot Turbo Base. After blotting the membranes were blocked in 5% skim milk solution and incubated with first antibody overnight. The membranes were washed three times with TBS+Tween20 and afterwards incubated with the peroxidase conjugated secondary antibody for one hour at room temperature. The chemiluminescence of the secondary antibody was activated using Immobilon Western Chemiluminsecent HRP Substrate (Millipore) and detected in the ChemiDoc™ XRS+ system (Bio-Rad Laboratories). Evaluation of the results was performed using Image Lab 5.2 Software (Bio-Rad Laboratories).

viii.Statistical analysis

Each experiment was repeated generally at least three times. Statistical significance of the difference between the examined values compared to the indicated control condition was determined by Student's *t*-test (paired or non-paired test dependent of the way of comparison) for the parametric data, or Mann-Whitney-U test for the non-parametric data. A P-value <0.05 was defined as significant.

3.3.3.3. Results

i. Binding of VEGFR2 to the its antibody

The results of immunocytochemistry show the staining of anti-VEGFR2 in/around RPE cells (Figure 12)

It suggest that the antibody may bind to at least the surface VEGFR2 and inhibit its function.

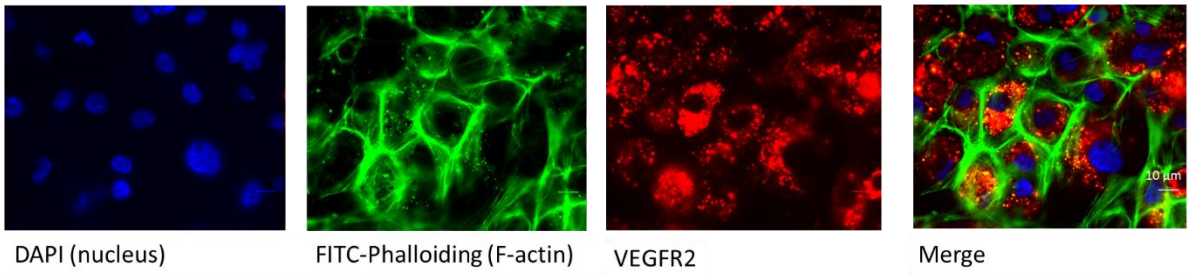

Fig. 12. Immunostaining of culture RPE cells with DAPI (blue), F-actin (green), and VEGFR2 (red). The right one is the merged image.

ii. VEGF secretion under inhibition of VEGFR2

VEGF secretion from RPE cells under inhibition of VEGFR2 was investigated under non-heated and sublethally-heated conditions. The results after 3h showed no difference in VEGF secretion in both cultures compared to the non-inhibited conditions (Fig. 13 A). After 24h, on the other hand, the secretion of VEGF was increased about 1.2 times compared to non-inhibited conditions in both cultures. These results suggest that anti-VEGFR2 may mildly increase VEGF secretion within 24h from RPE cells, but does not lead to the difference in VEGF secretion following sublethal heating.

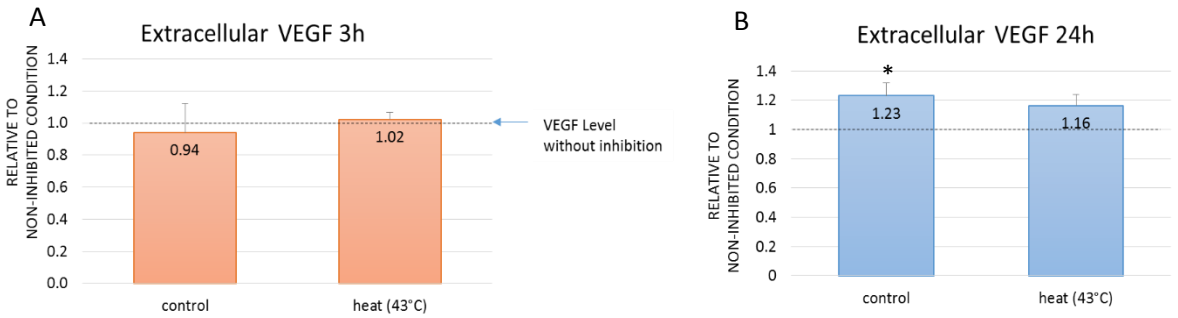

Fig. 13. Extracellular VEGF amount at 3h (A) and 24h (B) after irradiation (or sham irradiation), under inhibition of anti-VEGFR2. The antibody was added 2h before irradiation (or sham irradiation). The dash line is the VEGF level without VEGFR2 inhibition for each condition.

iii.Cell viability after sublethal hyperthermia under inhibition of VEGFR2

Cell viability after sublethal hyperthermia (T_{max}=40-59°C, from sublethal to lethal) was investigated with/without inhibition of VEGFR2. The results showed anti-VEGFR2 did not lead to any significant difference in cell viability (=percentage of living cells) up to 24h after irradiation (Fig. 14).

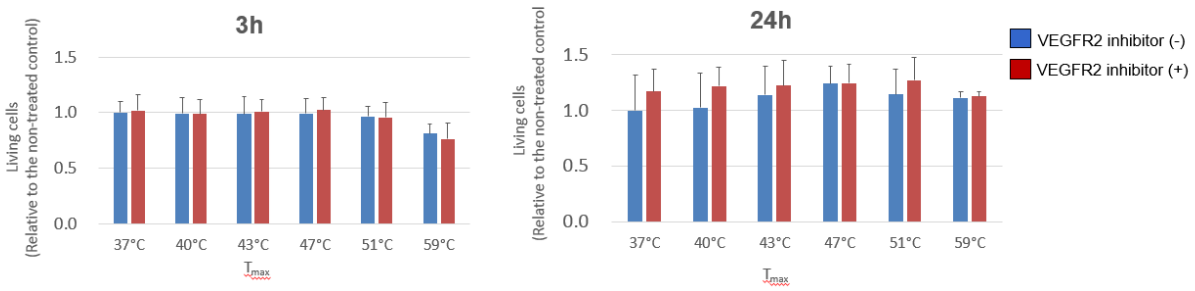

Fig. 14. Pre-treatment of anti-VEGFR2 did not alter RPE cell viability after laser irradiation.

iv.Heat shock protein 70 expression under inhibition of VEGFR2

Previous results (ref. annual reports 2016-2017) showed that intracellular Hsp70 was significantly increased especially after lethal irradiation (T_{max} ≥ 51°C with our irradiation setup), and sublethal irradiation also induces mild increase of this protein over 48h after irradiaiton. In this study, influence of VEGFR2 inhibition on heat-induced Hsp70 in RPE cells was investigated. Results showed that the increase of Hsp70 at 3h after irradiation was reduced in all temperature settings including sublethal heating (Fig. 15 A). After 24h, the difference was not obvious any more after sublethally irradiated cultures, bit there were still a large deviation of Hsp70 expression in lethally-irradiated cultures (Fig. 15 B). These results suggest that inhibition of VEGFR2 suppress the heat-induced expression of Hsp70 in RPE cells after thermal laser irradiation.

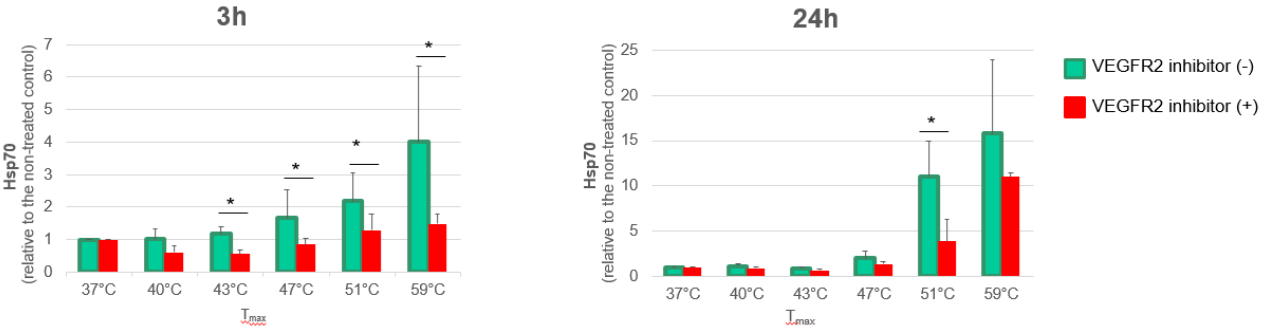

Fig. 15. Hsp70 expression in RPE cells without VEGFR2 inhibition (green) and with inhibition (red) after laser-induced hyperthermia with different T_{max}.

3.3.3.4. Discussion

The results that VEGFR2 inhibition reduced heat-induced expression of Hsp70 strongly suggest that 1) VEGF-A/VEGFR2 signaling is activated by RPE hyperthermia, and 2) VEGF-A/VEGFR2 signaling positively regulate Hsp70 expression under heat-induced cell stress. Taking together with the previous result reported last year, that inhibition of Hsp70 significantly increased the expression of intracellular VEGF, Hsp70 may negatively regulate the VEGF-A production after thermal stress. The figure below is our hypothesis, a regulatory cycle between heat induced VEGF-A autocrine/VEGFR2 pathway and Hsp70. Under inhibition of VEGFR2, as simulated in this experiment, their positive regulation of Hsp70 expression may be suppressed, and moreover, it might also suppress VEGF-indced mitochondrial biogenesis.[7] Since ATP is an essential cofactor of Hsp70, not only amount but also the functionality of Hsp70 is considered to be reduced by the inhibition of VEGF-A/VEGFR2 pathway.

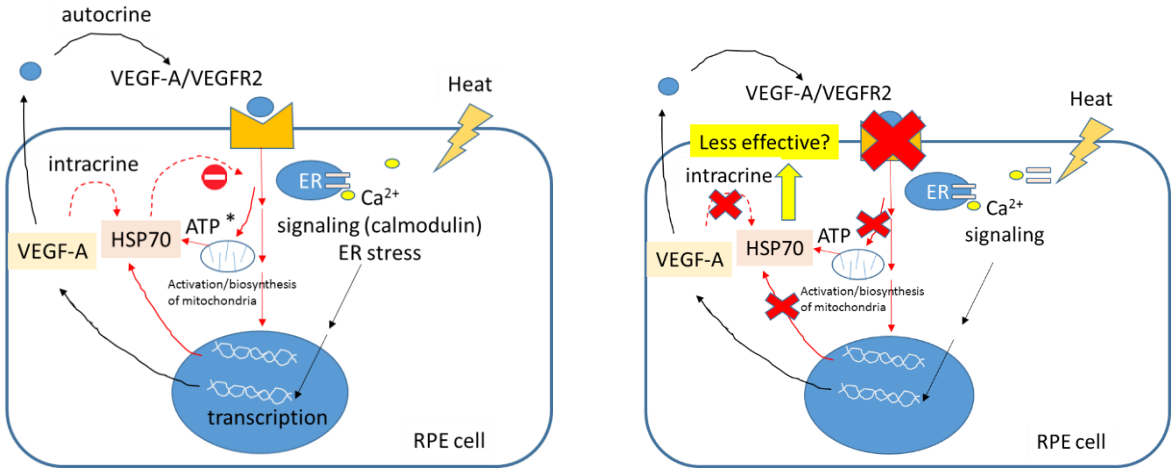

Fig. 16. Schematic description of our hypothesis for bilateral regulations between VEGF-A/VEGFR2 signaling and Hsp70 in RPE cells under heat stimulation. (left) no VEGFR2 inhibition, (right9 with VEGFR2 inhibition. Under VEGFR2 inhibition, effect of Hsp70 can be less than under un-inhibited conditions.

Since the induced expression of Hsp70 by thermal laser irradiation is essential to protect cells from thermal stress and in the functional remodeling of RPE cells after sublethal hyperthermia, the inhibitory condition of VEGF-A/VEGFR2 might negatively affect sublethal PRE laser treatment. In the clinical practice, therefore, according to the current results, laser irradiation directly after anti-VEGF treatment might be better avoided for the most therapeutic effect of thermal treatment. Further detailed basic and clinical study is needed to prove this hypothesis and to understand mechanisms more indetail about the regulatory system between VEGF and Hsp70.

3.4. WP5: Effect of thermal laser irradiation of RPE cell functionality

As one of the functionalities, effect of sublethal hyperthermia on the wound healing of monolayer RPE was investigated.

3.4.1. Method

Porcine RPE cells were cultured in the special culture dish for wound healing assay, provided by ibidi (Culture-Insert 3 Well in µ-Dish 35 mm, high). This culture dish has a 3-well silicone insert with two defined cell-free gaps. Silicone insert may be easily removed from the glass bottom with forceps. After the cell culture becomes confluent in the cell growing area, the silicone insert can be carefully removed, so that the cells are allowed to grow into the cell-free space (Fig. 17). In this experiment, some cultures were irradiated sublethally with thulium laser (T_{max}=40°C and 45°C), and the "wound closure" was compared among conditions after 24h. The initial width of the wound is 500 µm. The mean width of the wound after 24h was measured with image J.

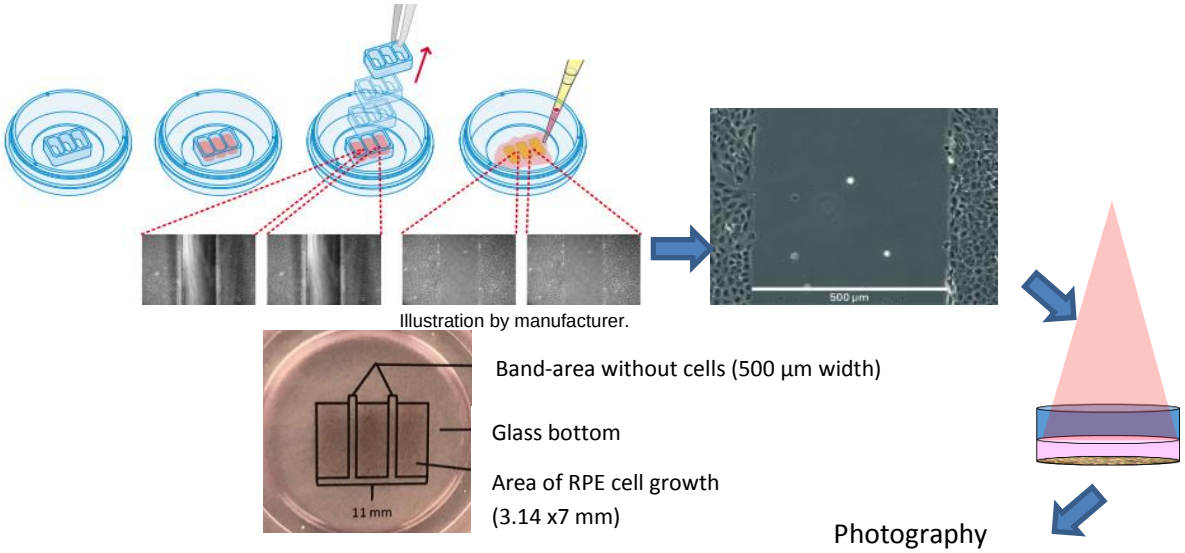

Fig. 17. Experimental flow of wound healing assay.

3.4.2. Results

The wound width after 24h was significantly smaller in the culture irradiation sublethally with T_{max}=40°C and 45°C (Fig. 18 A upper images, Fig. 18 B). Result of the detection of proliferating cells with EdU revealed that cell proliferation was significantly increased in the culture irradiated with T_{max}=40°C, but not 45°C (Fig. 18 A lower images, Fig. 18 C). These results suggest that sublethal hyperthermia may stimulate RPE cell proliferation and/or migration. By irradiation with T_{max}=45°C wound healing was accelerated without increasing cell proliferation,

suggesting that the RPE wound closure after irradiation with T_{max}=45°C was accelerated through the stimulation of cell migration.

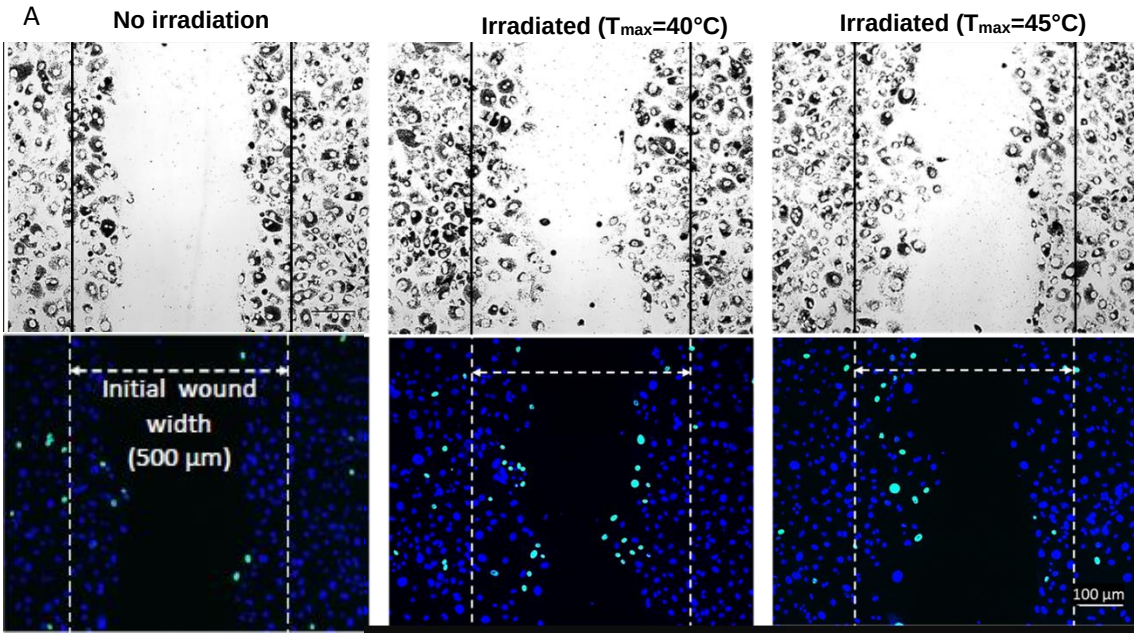

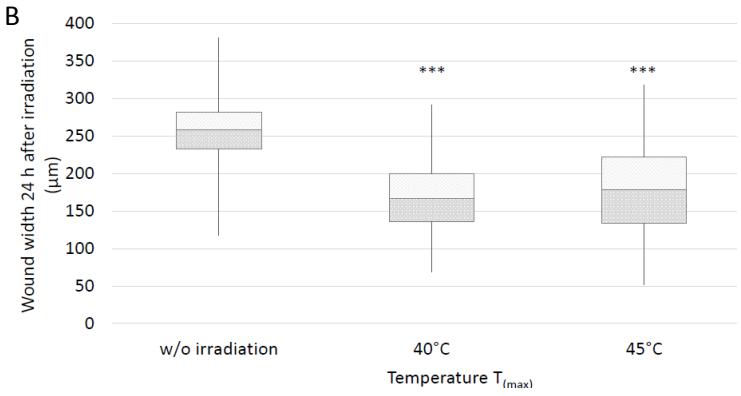

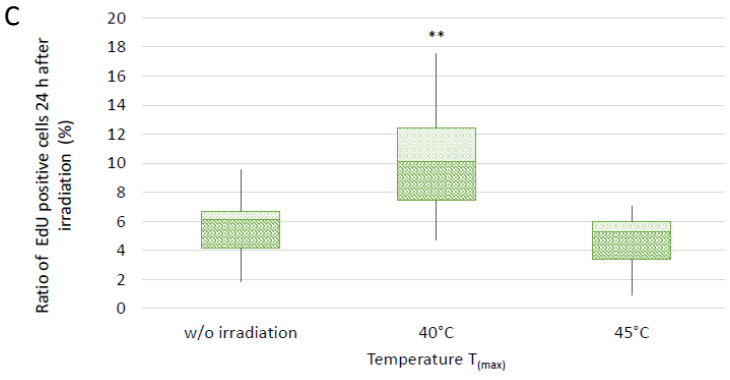

Fig. 18. Results of RPE wound healing assay.

A) (upper) Phase contrast microscopy image of RPE cells at the wound after 24h. (lower) EdU (green) and DAPI (blue) staining at the same location. EdU-positive indicates cell division. DAPI indicates cell nucleus of all cells.

B) Wound width after 24h. The wound width of the irradiated cultures was significantly smaller than of the non-irradiated culture. (*** p<0.0001)

C) The percentage of proliferating cells (EdU positive cells) in the examined area after 24h. The number of EdU positive cells was significantly higher in the culture irradiated with T_{max}=43°C. (**p<0.01)

3.4.3. Discussion

The results of wound healing assay as well as viability assay suggest that sublethal hyperthermia, even for 10s, may stimulate cell proliferation and/or migration of RPE cells. In vivo, RPE cell proliferation is not necessary as long as the RPE keeps monolayer with integrated tight junctions. However, there are some situations, in which RPE cell proliferation is required for tissue restoration, for example in case of RPE defect caused by a wound by surgery or in the eye with localized RPE atrophy. Those pathological conditions could be ones of the therapy indications of sublethal RPE hyperthermia. With respect to cell migration, negative impact of the activated migration through transformation of cells from epithelial to mesenchymal phenotypes (EMT: epithelial mesenchymal transition) are to be taken into consideration. EMT is considered to be one of the cell alterations toward AMD[8], because many migrating RPE cells are observed in the retina or sub-retinal space in the eyes of dry AMD.[9] Therefore, the use of the temperature or thermal dose that might stimlate EMT domoinantly should be probably avoided for the tretament of AMD or pre-AMD. The exact temperature or thermal dose for that has, however, not been elucidate yet to date.

4. Summary (whole project)

1. **In vitro optoacoustic temperature measurements on RPE hyperthermia model**
   The first model has been completed in the end of 2018, feasibility has been proven and the data was published.

2. **Investigation of the accuracy of temperature measurement with two different techniques**
   During the visit of our scientist to the laboratory of AFRL, our optoacouostic method was installed in the AFRS laboratory and simltaneous measurements with a fast IR camera proved the OA technique. Further first measurements with melanin loaded cells also shows high temperature accordance among both techniques. However, even though the average values correlate strongly, the signal to noise ratio of the OA measurement needs to be improved with respect to obtain lower pulse to pulse fluctuations and higher accuracy. As a first step, the pulse to pulse fluctuations of the laser need to be reduced or the signal to be normalized to it.

3. **Investigation of damage kinetics after thermal laser irradiation**
   Damage kinetics following short-term laser-induced temperature increase for the time range from a few hours to days have been shown. Apoptotic cell death pathway has been shown to take place mostly in thermal laser-induced late cell death.

4. **Investigation of intracellular signaling and proteostasis after thermal laser irradiation**
   Different types of thermal impact-dependent intracelllar signaling and protein expression have been elucidated; particularly insights into the role of Hsp70, calcium flow, VEGF expression and reglation between Hsp70 and VEGF under sublethal hyperthermia have been proven.

5. **Investigation of long-term cellular functionality after thermal laser irradiation**
   Antioxidative effect and enhancing effect of wound healing of RPE cells have been shown.

Conclusion

In contrast to the clear exogenous determinant of cell death following thermal stimulation (=temperature x time), endogenous determinant seems to be a complexed, highly-regulated intracellular control system involving different proteins and molecules. Hsp70, which had been assumed to be one of the dominant determinants, also seems to be regulated by other different signaling pathways and their depletion was compensated at least for a short time period, up to a few days after stimulation. This regulation system

might be different amoung cell types, for example, between healty cells and cancer cells, which should be compared under same thermal stress. Using our new method to heat cultured cells with a real-time temperature measurement, the threshold temperature for cell death and further intracellular regulatory system may be elucidated under better control and monitoring of temperature increase.

Involvement of Hsp70, VEGF, and Thioredoxin in heat-induced cellular response in RPE cells were clearly shown. Elucidating their mutual regulation system is considered to be a key to understand cellular response to therapeutic sublethal hyperthermia.

5. Literatures

1. GW F, GA S, MA H, SB W, DC T,S P. Vascular endothelial growth factor-A regulation of blood vessel sprouting in health and disease. *. OA Biochemistry.* 2013;1:5.
2. Nguyen CL, Oh LJ, Wong E, Wei J,Chilov M. Anti-vascular endothelial growth factor for neovascular age-related macular degeneration: a meta-analysis of randomized controlled trials*. BMC Ophthalmol.* 2018;18:130.
3. Byeon SH, Lee SC, Choi SH, et al. Vascular Endothelial Growth Factor as an Autocrine Survival Factor for Retinal Pigment Epithelial Cells under Oxidative Stress via the VEGF-R2/PI3K/Akt*. Investigative Ophthalmology & Visual Science.* 2010;51:1190-1197.
4. Bhisitkul RB, Mendes TS, Rofagha S, et al. Macular atrophy progression and 7-year vision outcomes in subjects from the ANCHOR, MARINA, and HORIZON studies: the SEVEN-UP study*. Am J Ophthalmol.* 2015;159:915-924 e912.
5. Mehta H, Gillies MC,Fraser-Bell S. Combination of vascular endothelial growth factor inhibitors and laser therapy for diabetic macular oedema: a review*. Clin Exp Ophthalmol.* 2016;44:335-339.
6. Safari E, Zavaran Hosseini A, Hassan Z, Khajeh K, Ardestani MS,Baradaran B. Cytotoxic Effect of Immunotoxin Containing The Truncated Form of Pseudomonas Exotoxin A and Anti-VEGFR2 on HUVEC and MCF-7 Cell Lines*. Cell J.* 2014;16:203-210.
7. Wright GL, Maroulakou IG, Eldridge J, et al. VEGF stimulation of mitochondrial biogenesis: requirement of AKT3 kinase*. FASEB J.* 2008;22:3264-3275.
8. Ghosh S, Shang P, Terasaki H, et al. A Role for betaA3/A1-Crystallin in Type 2 EMT of RPE Cells Occurring in Dry Age-Related Macular Degeneration*. Invest Ophthalmol Vis Sci.* 2018;59:AMD104-AMD113.
9. Sarks JP, Sarks SH,Killingsworth MC. Evolution of Geographic Atrophy of the Retinal-Pigment Epithelium*. Eye.* 1988;2:552-577.

6. Performance reports (conference presentation, publication) (whole project period)

Main Members for the project 2017-2018

PI: Yoko Miura, Ralf Brinkmann

Doctoral student: Katharina Kern, Eric Seifert

Engineer: Josua Rehra, Dirk Theisen-Kunde, Nicolas Ditrez

Conference presentations

May 2019: ARVO (Association for Research in Vision and Ophthalmology) annual meeting. **"**Sublethal hyperthermia on retinal pigment epithelium -possible role of heat shock protein 70 and influence of the inhibition of vascular endothelial growth factor-mediated signaling." Y. Miura, K. Kern, R. Brinkmann. Vancouver, Canada

Dec 2018: J-SMILE meeting (Japaneses society of minimally invasive retina laser therapy) "Basic of minimally invasive retinal laser –mechanism of action and cell responses." Y. Miura. Tokyo Japan

Oct 2018: LIGHT meeting (annual meeting of International retina laser society) in Chicago. "Influence of the inhibition of VEGF receptor 2 on the responses of cultured RPE cells to the laser-induced sublethal hyperthermia" Y. Miura, K. Kern, E. Seifert, R. Brinkmann. Chicago, USA

May 2018: ARVO (Association for Research in Vision and Ophthalmology) annual meeting. "Comparison and Analysis of Micropulse and Continuous Wave Laser Application on Retinal Pigment Epithelium (RPE) ex vivo." R. Brinkmann, K. Inagaki, B. Schmarbeck, A. Hutfilz, K. Bliedtner, K. Ohkoshi, Y. Miura. Honolulu, USA

May 2018: ARVO (Association for Research in Vision and Ophthalmology) annual meeting. "Influence of thermal laser irradiation on cell proliferation and wound healing of primary RPE cell cultures." K. Kern, R. Schaefer, C.I. Mertineit, R. Brinkmann, Y. Miura. Honolulu, USA

May 2017: ARVO (Association for Research in Vision and Ophthalmology) annual meeting "Influence of the TRPV-1 channel and HSP70 on RPE cell survival after transient temperature rise." K. Kern, S. Beier, R. Brinkmann, Y. Miura. Baltimore, USA

Nov 2016: Life Sciences Review

Cell response determinants in laser-induced thermal impacts. Y. Miura, R. Brinkmann. Dayton, USA

Sep 2016: DOG (German Ophthalmology Congress)
Die Rolle von HSP70 bei Hyperthermie des retinalen Pigmentepithels - Implikationen für die thermische Stimulation der Retina (Role of Hsp70 in RPE hyperthermia -implication for the thermal stimulation of the retina). K. Kern, C.L. Matrineit, S. Beier, J. Pruessner, R. Brinkmann, Y. Miura. Berlin, Germany

Publications

1) Y. Miura, E. Seifert, J. Rehra, K. Kern, D. Theisen-Kunde, M. Denton, R. Brinkmann: ***Real-time optoacoustic temperature determination on cell cultures during heat exposure: a feasibility study.*** Int J Hyperth, pp. 1-7, 2019

2) K. Kern, C.L. Mertineit, R. Brinkmann, Y. Miura
Expression of heat shock protein 70 and cell death kinetics after different thermal impacts on cultured retinal pigment epithelial cells
Exp Eye Res, no. 170, pp. 117-126, 2018

3) Y. Miura, J. Pruessner, C.L. Mertineit, K. Kern, M. Muenter, M. Moltmann, V. Danicke, R. Brinkmann. ***Continuous-wave Thulium Laser for Heating Cultured Cells to Investigate Cellular Thermal Effects.*** J Vis Exp. 30;(124), 2017

Abstracts
1) **"Sublethal hyperthermia on retinal pigment epithelium -possible role of heat shock protein 70 and influence of the inhibition of vascular endothelial growth factor-mediated signaling."** Y. Miura, K. Kern, R. Brinkmann. *Invest. Ophthalmol. Vis. Sci..* 2019;

2) **"Comparison and Analysis of Micropulse and Continuous Wave Laser Application on Retinal Pigment Epithelium (RPE) ex vivo."** R. Brinkmann, K. Inagaki, B. Schmarbeck, A. Hutfilz, K. Bliedtner, K. Ohkoshi, Y. Miura. *Invest. Ophthalmol. Vis. Sci..* 2018; 59(9):6199

3) **"Influence of thermal laser irradiation on cell proliferation and wound healing of primary RPE cell cultures."** K. Kern, R. Schaefer, C.l. Mertineit, R. Brinkmann, Y. Miura. Invest. Ophthalmol. Vis. Sci.. 2018; 59(9):4004.

7. List of Symbols, Abbreviations and Acronyms

DMEM: Dalbecco's modified eagle's medium
DMSO: Dimethyl sulfoxide
ELISA: enzyme-linked immunosorbent assay
EMT: epithelial mesenchymal transition
EthD-III: ethidium homodimer III
FITC: Fluorescein isothiocyanate
Hsp70: heat shock protein 70
OA: optoacostic
PBS: phosphate buffered saline
PVDF: Polyvinylidene fluoride
RPE: retinal pigment epithelium
TRPV1: transient receptor potential cation channel subfamily V member 1
VEGF: vascular endothelial growth factor
VEGFR2: vascular endothelial growth factor receptor 2